Optik 126 (2015) 1445–1448

Contents lists available at ScienceDirect

Optik

journal homepage: www.elsevier.de/ijleo

Spatial measurement of ultrashort light pulses using two photon absorption in a colliding geometry

Federico E. Sanjuan [a,b,*], Borja Vidal [a]

[a] Nanophotonics Technology Center, Universitat Politècnica de València, Camino de Vera, s.n., ES-46022 Valencia, Spain
[b] Optical Research Center (Conicet-CIC), Camino Centenario y 506, 1897, La Plata, Buenos Aires, Argentina

ARTICLE INFO

Article history:
Received 3 March 2014
Accepted 14 April 2015

Keywords:
Autocorrelator
Interferometer
TPA

ABSTRACT

In this work the spatial measurement of ultrashort light pulses through two photon absorption (TPA) is analyzed. The method is based on a Michelson interferometer configuration in a colliding geometry where the light pulses meet each other in a cell with Rhodamine B in ethanol, which emits a fluorescence that can be detected with a standard digital camera. The analysis of the experimental spatial trace as well as the theoretical derivation show that the Full Width at Half Maximum (FWHM) measured is $FWHM_{measured} = FWHM_{single\_pulse}/\sqrt{2}$ instead of the general value $\sqrt{2}$ $FWHM_{single\_pulse}$ of temporal or spatial collinear approaches. The influence of the pulse chirp on the measurement and the error caused by the camera misalignment are analyzed.

1. Introduction

Through the last decades laser pulses have been decreasing the temporal width reaching in the actuality up to attosecond duration [1]. Laser pulses ranging from a few femtoseconds to a few hundred femtoseconds are reliably produced through different mode-locking techniques [2,3], which have been used to study a wide range of ultrafast phenomena [4]. The temporal characterization of these laser pulses is an important aspect of such investigations to understand the dynamics of the processes involved. Therefore several techniques such as intensity autocorrelation [5,6], third order autocorrelation [7], frequency resolved optical gating (FROG) [8] and many others have been developed.

Nonlinear autocorrelation has been implemented mainly using two techniques that are described as follows.

Second order autocorrelation (based on Second Harmonic Generation, SHG) [9,10] is based on a medium with high second-order nonlinear susceptibility [11]. In order to measure the pulse, this technique requires a phase matching and a sensitive detector, typically a photomultiplier.

The other method relies on two photon absorption (TPA) [12], i.e. the absorption of two coherent photons as a consequence of a third order nonlinear process [9].

These processes are sensitive to compression of optical power in time and in space domains because of its nonlinear nature. Especially the sensitivity of the TPA process to the compression of optical power in time has widely been used to build systems for autocorrelation [13], cross-correlation [14], measurement of very short pulses with TPA photoconductivity [12], and even for optical communication applications.

There are two approaches for TPA-based pulse measurements: observing the change in the transmission or luminescence in a material; and measuring the charge generated by the nonlinear absorption of the light.

Different interferometer configurations for measuring laser pulse widths using TPA have been tested, as described in [15], where a review of the different approaches is provided. Many schemes are based on a temporal or spatial analysis [16–18], where by delaying an arm of the interferometer, a temporal or spatial trace of the TPA emission is mapped with different detectors like densitometers, photomultipliers, etc.

In this work, an analysis of a spatial autocorrelation setup based on the TPA-induced fluorescence in an organic dye solution (Rhodamine B in ethanol) using a Michelson interferometer in a colliding configuration is presented. A theoretical analysis has been carried out, including the pulse chirp. Experimental results validate the analysis and show the difference between the colliding spatial configuration and other approaches. Finally, a calibration method and the influence of the camera misalignment are discussed.

* Corresponding author at: Optical Research Center (Conicet-CIC), Camino Centenario y 506, 1897, La Plata, Buenos Aires, Argentina. Tel.: +54 2214840280; fax: +54 2214712771.
E-mail addresses: fedesanjuan@yahoo.com.ar (F.E. Sanjuan), bvidal@dcom.upv.es (B. Vidal).

http://dx.doi.org/10.1016/j.ijleo.2015.04.027
0030-4026/

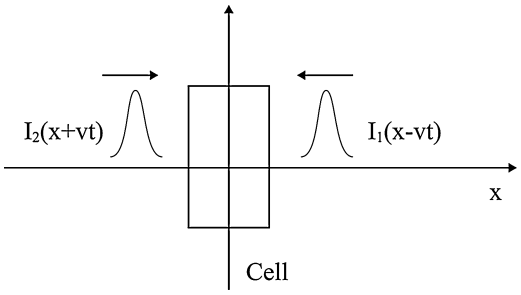

Fig. 1. Pulses configuration in a colliding geometry.

2. Theory

A theoretical analysis is developed for pulses in a colliding geometry (Fig. 1), which will be temporal overlapped in a cell with Rhodamine B in ethanol.

The intensity dissipation caused by two photon absorption in the cell is [9],

$$\frac{\partial I}{\partial X} = \beta \left|E_0\right|^4 \tag{1}$$

where E_0 is the electric field and $\beta = (3/2\varepsilon_0 n^2 c^2)\omega\chi_{xxxx}$, χ is the susceptibility, ω the angular laser frequency, n the refractive index, c is the light velocity and ε_0 the vacuum permittivity.

The electric fields of the two pulses in a colliding configuration can be described as,

$$E_0(y,z,x-vt) = E_1(y,z,x-vt)e^{-i(kx-\vartheta_1)} + E_2(y,z,x+vt)e^{i(kx+\vartheta_2)} \tag{2}$$

where v is the propagation velocity of the electric field and k is wave vector.

Substituting Eq. (2) into Eq. (1),

$$\frac{\partial I}{\partial x}(y,z,x-vt) = \beta \begin{pmatrix} E_1^4(y,z,x-vt) + E_2^4(y,z,x+vt) + \\ +4E_1^3(y,z,x+vt)E_2(y,z,x-vt)\cos(2kx+\vartheta_2-\vartheta_1) + \\ +4E_1(y,z,x-vt)E_2^3(y,z,x+vt)\cos(2kx+\vartheta_2-\vartheta_1) + \\ +4E_1^2(y,z,x-vt)E_2^2(y,z,x+vt) + \\ +2E_1^2(y,z,x-vt)E_2^2(y,z,x+vt)\cos(4kx+2(\vartheta_2-\vartheta_1)) \end{pmatrix} \tag{3}$$

The third, fourth and last term of Eq. (3) have a spatial modulation that cannot be resolved by the digital camera. So Eq. (3) leads to,

$$\frac{\partial I}{\partial x}(y,z,x-vt) = \beta\left(E_1^4(y,z,x-vt) + E_2^4(y,z,x+vt) + 4E_1^2(y,z,x-vt){E_2}^2(y,z,x+vt)\right) \tag{4}$$

The relationship between the electric field and the pulse intensity is given by,

$$I = \frac{\varepsilon_0 cn}{2}\left|E_0\right|^2 \tag{5}$$

By inserting Eq. (5) into Eq. (4), an intensity dependence result is achieved,

$$\frac{\partial I}{\partial x}(y,z,x-vt) = \delta\left(I_1^2(y,z,x-vt) + I_2^2(y,z,x+vt) + 4I_1(y,z,x-vt)I_2(y,z,x+vt)\right) \tag{6}$$

Integrating over the cross sectional coordinates z and y and also integrating in time, Eq. (6) gives the solution of the spatial trace. Assuming that I_1 and I_2 in Eq. (6) are one dimensional Gaussian pulses propagating in the x direction with the same amplitude and opposite directions,

$$I_1 = e^{-(x-vt)^2} \tag{7}$$

$$I_2 = e^{-(x+vt)^2} \tag{8}$$

Substituting Eqs. (7) and (8) into Eq. (6) and integrating the expression in time, we obtain

$$\int_{-\infty}^{\infty} I_2^2 dt = \int_{-\infty}^{\infty} I_1^2 dt = \int_{-\infty}^{+\infty} e^{-2(x-vt)^2} dt = \frac{\sqrt{\pi}}{v\sqrt{2}} \tag{9}$$

$$4\int_{-\infty}^{+\infty} I_1 I_2 dt = 4\int_{-\infty}^{+\infty} e^{-(x-vt)^2} e^{-(x+vt)^2} dt = 4e^{-2x^2}\int_{-\infty}^{+\infty} e^{-2(vt)^2} dt = \frac{4\sqrt{\pi}e^{-2x^2}}{\sqrt{2}v} \tag{10}$$

Applying the result of the integrals (9) and (10) to (6),

$$S(x) = \frac{\partial I}{\partial x}(x) = \delta\left(\frac{2}{v}\sqrt{\frac{\pi}{2}} + \frac{4\sqrt{\pi}e^{-2x^2}}{\sqrt{2}v}\right) \tag{11}$$

From Eq. (11) we can observe in the second term that the result is a Gaussian function with smaller variance in comparison to the original pulse. It can also be seen that there is a constant value (first term) caused by the independent interaction of the dye solution with the laser pulses. In consequence the measured Full Width at Half Maximum (FWHM) is,

$$\mathrm{FWHM}_{\mathrm{measured}} = \frac{\mathrm{FWHM}_{\mathrm{single\_pulse}}}{\sqrt{2}} \tag{12}$$

The contrast obtained when both pulses have the same amplitude, is [17],

$$\frac{S(0)}{S(\infty)} = 3 \tag{13}$$

The factor in the FWHM relation of (13) changes depending on the pulse shape (e.g. 1.54 for a sech^2).

3. Numerical simulation

Numerical simulations have been carried out using Eq. (1) assuming two Gaussian pulses with the same amplitude propagating in x direction where a linear chirping is considered. Hence Eq. (2) becomes,

$$E_0(x,t) = e^{\frac{2\ln 2}{a^2}(x-vt)^2}\sin\left(nkx - (wt+\pi bt^2)\right) + e^{-\frac{2\ln 2}{a^2}(x+vt)^2}\sin(nkx+wt+\pi bt^2) \tag{14}$$

Assuming $c = 0.3$ μm/fs, $n_{\mathrm{ethanol}} = 1.361$, $\lambda_{\mathrm{laser}} = 0.8$ μm, $b = 0$, $k = 2\pi/\lambda$, $\omega = ck$, $a = (c/n)T$, T = 123.8 fs, and $v = c/n$.

The spatial intensity dissipation caused by two photon absorption in the cell is obtained as,

$$S(x) = \int_{-\infty}^{\infty} (E_0(x,t))^4 dt \tag{16}$$

In Fig. 2a the electrical field is observed. However, the camera resolution does not allow the observation of these high frequency oscillations. To reflect this fact in the simulation, we made the convolution between $S(x)$ and a Gaussian pulse width equal to the

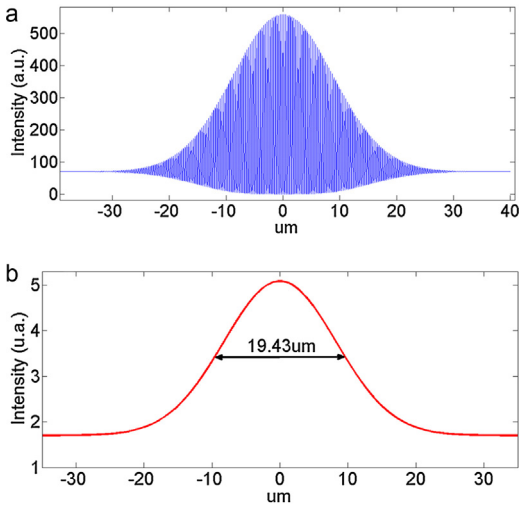

Fig. 2. (a). Result of Eq. (16). (b) Result of the convolution of (a) with a Gaussian function of FWHM = 1.145um (camera resolution).

spatial resolution of the camera (2.29 μm) used in the experiment (Fig. 2b).

Making a fitting with a Gaussian function in Fig. 2b, we obtain a FWHM = 19.43 μm, which gives a temporal width of 124.65 fs. The contrast between the peak of the signal and the back is three, which is in agreement with theory.

Decreasing the resolution of the camera, the obtained pulse width is closer to the theoretical value (19.31 μm).

Chirp in the pulses is simulated by making $b \neq 0$ in Eq. (14). The effect of pulse chirp on the autocorrelation setup has been analyzed using an instantaneous frequency value of $f(t) = f_0 - (t50 * 10^{-6}/fs^2)$. It corresponds with the chirp value of the laser used in the experimental setup measured with the FROG technique.

The simulation shows no changes in Fig. 2b, even when the chirping was incremented one order of magnitude.

4. Experiment

The experimental setup sketched in Fig. 3 was used to validate the analysis. The pulses were obtained from a mode locked Ti:Sapphire laser, with 80 MHz frequency rate, 1 W average power, 800 nm wavelength, and 124 fs pulse duration (MAI TAI, Spectra Physics). Fig. 3 shows a Michelson interferometer in a colliding configuration with a stepper motor in the delay line and a cell with Rhodamine B in ethanol where the pulses are temporal overlapped.

To avoid light scattering in the cell caused by the interaction of dust particles with the laser (Fig. 4), a filter in front of the camera to remove the 800 nm laser wavelength has been used. Since the

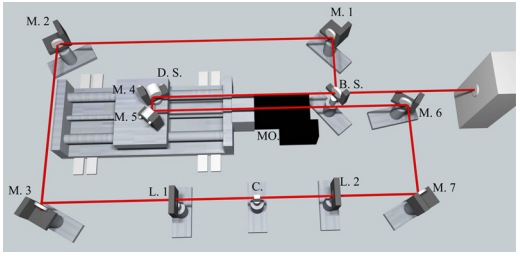

Fig. 3. Configuration of the Michelson spectrometer; M.1, M.2, M.3, M.4, M.5, M.6, M7 are the mirrors; B.S. is the beam splitter; L.1, L2 are the lens with 5 cm focal distance; D.S. is the delay stage, MO. is the stepper motor; C. is the cell with Rhodamine B where the pulses overlapped.

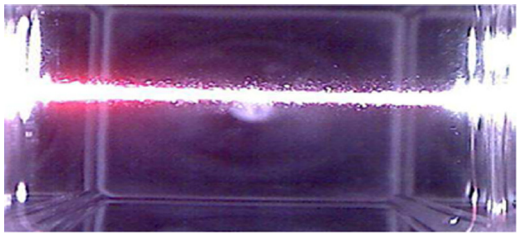

Fig. 4. Photograph with scattering presence.

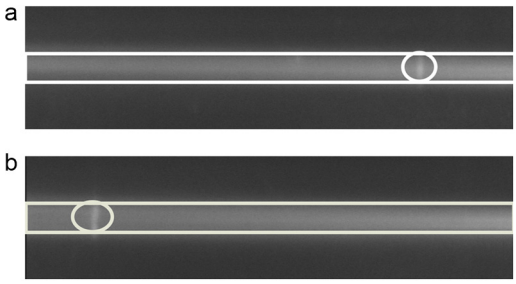

Fig. 5. (a), (b). Images of two different places of the temporal overlapped pulses.

fluorescence emission of Rhodamine B is close to 600 nm [19], the filter does not affect the desired signal.

The image is captured with a commercial camera (Sony DSC-H9). In Fig. 5 the spatial measurement is shown for two different delay line positions.

4.1. Results

In order to improve the quality of the image and increment the signal to noise ratio, we made a spatial average in the rectangle shown in Fig. 5a and 5b, obtaining Fig. 6 by adding both images.

The contrast between the peak and the background is 1.2. It is less than the theoretical value, 3 [17], because we did not have the same laser intensity in each arm of the interferometer and they are not perfectly overlapped.

Calibration is needed to know the pixel length. In order to obtain the pixel/length ratio, we first took a picture in a certain position (Fig. 5a) where the pulses are temporal overlapped. Then, we moved the motor a number of steps equivalent to a length L, and we take a new picture (Fig. 5b). From these, we obtained the scale, because the number of pixels between the peaks shift is equal to L/n_{ethanol} (see Fig. 6), and the camera resolution.

By fitting with a Gaussian function the fluorescence of the overlapped pulses from Fig. 5a, a FWHM of 19.46 μm (Fig. 7) is obtained. Applying Eq. (12) gives, $\text{FWHM}_{\text{single-pulse-temp}} = \text{FWHM}_{\text{measured}}\sqrt{2}(n/c) = 124.85$ fs

To validate the performance of the autocorrelator, the pulses were also measured using a commercial FROG instrument,

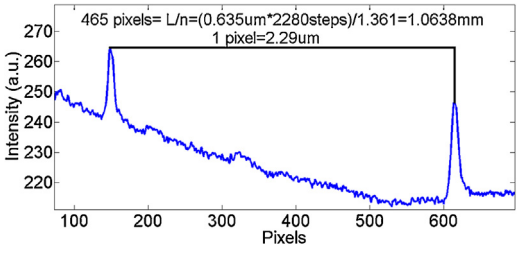

Fig. 6. Spatial average of the two images sum.

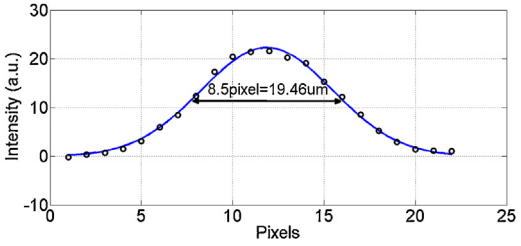

Fig. 7. Dots are the measure fluorescence and in solid line there is a fitting by a Gaussian function.

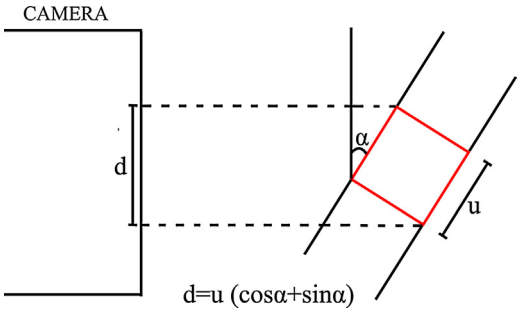

Fig. 8. Camera misalignment; u is the pulse width, α is the angle between the cell and the camera, and d is the ray projection onto the camera.

obtaining 123.8 ± 0.02 fs, which is similar to the experimental result by our method.

4.2. Error analysis

The spatial measurement technique is sensitive to error due to the misalignment between the cell and the orthogonal camera, as shown in Fig. 8, where is assumed for simplicity that the intensity is constant in the overlapping area, i.e. it is a rectangle. The projection onto the camera, d, can be achieved through ray projection,

$$d = u(\cos\alpha + \sin\alpha) \tag{17}$$

where u is the pulse width and α is the angle between the cell and the camera.

Eq. (17) shows that since always $d \geq u$, any misalignment will increase the pulse width. For example $\alpha = 5^\circ$ increases the pulse width in an 8.3%.

Another source of error in the measurement comes from the camera resolution. In particular, in the experiment it was $\pm 1.145\ \mu m = \pm 5.2$ fs.

There is no evidence of pulse dispersion caused by the ethanol or from the polypropylene cell. For laser pulse widths smaller than 1 fs, the spectral bandwidth of Rhodamine B should be taken into account.

5. Conclusions

In this paper we have described a spatial analysis for measuring ultrashort light pulses using two photon absorption in a colliding geometry. It has been shown both theoretical and experimentally that the spatial pulse width measured with Gaussian pulses is $FWHM_{measured} = FWHM_{single\_pulse}/\sqrt{2}$, which leads to a result different from the classic temporal or spatial collinear analysis where the autocorrelation gives $FWHM_{measured} = FWHM_{single\_pulse}\sqrt{2}$ [16–18]. A method to calibrate the system using a commercial camera has also been analyzed. The experimental results agree with the numerical and theoretical analysis with an uncertainty of 5 fs. Chirp has also been taken into account showing no influence in the pulse measurement. Finally, an analysis of the camera misalignment has also been provided.

Acknowledgments

The work was partially supported by a PME-2006-00018 (Equipment Modernization Project for research laboratories, 2006) grant from Agencia Nacional de Investigaciones Científicas y Tecnológicas del Ministerio de la investigación, ciencia e innovación de la nación (Argentina). The authors thank the contribution of Dr. Gustavo Torchia to the academic development of Federico Sanjuan.

References

[1] J. Carrera, X.M. Tong, S. Chu, Creation and control of a single coherent attosecond xuv pulse by few-cycle intense laser pulses, Phys. Rev. A 74 (2006) 0234034.
[2] K.X. Liu, C.J. Flood, D.R. Walker, H.M. Van Driel, Kerr lens mode locking of a diode-pumped Nd:YAG laser, Opt. Lett. 17 (1992) 1361–1363.
[3] I.P. Bilinsky, J.G. Fujimoto, J.N. Walpole, L.J. Missaggia, Semiconductor doped silica saturable absorber films for solid-state laser mode locking, Opt. Lett. 23 (1998) 1766–1768.
[4] D. Mcmorrow, W.T. Lotshaw, G.A. Kenney Wallace, Femtosecond optical Kerr studies on the origin of the nonlinear responses in simple liquids, Quantum Electron. 24 (1988) 443–454.
[5] Z.A. Yasa, N.M. Amer, A rapid scanning autocorrelation scheme for continuous monitoring of picosecond laser pulses, Opt. Commun. 36 (1981) 406–408.
[6] J.H. Chung, A.M. Weiner, Ambiguity of ultrashort pulse shapes retrieved from the intensity autocorrelation and the power spectrum, Quantum Electron. 7 (2001) 656–666.
[7] J. Etchepare, G. Grillon, A. Orszag, Third order electronic susceptibilities of liquids measured by femtosecond kinetics of optical Kerr effect, Quantum Electron. 19 (1983) 775–778.
[8] R. Trebino, Frequency Resolved Optical Gatin: The Measurements of Ultrashort Laser Pulses, Kluwer Academic Publishers, USA, 2000.
[9] R. Salem, Master Thesis, University of Maryland, College Park, 2003.
[10] M. Raghuramaiah, A.K. Sharma, P.A. Naik, P.D. Gupta, R.A. Ganeev, A second-order autocorrelator for single-shot measurement of femtosecond laser pulse durations, Sadhana (2001) 1603–1611.
[11] P.A. Franken, A.E. Hill, C.W. Peters, G. Weinreich, Generation of optical harmonics, Phys. Rev. Lett. 7 (1961) 118–119.
[12] A.M. Streltsov, J.K. Ranka, A.L. Gaeta, Femtosecond ultraviolet autocorrelation measurements based on two-photon conductivity in fused silica, Opt. Lett. 23 (1998) 798–800.
[13] D.T. Reid, W. Sibbett, J.M. Dudley, L.P. Barry, B. Thomsen, J.D. Harvey, Commercial semiconductor devices for two photon absorption autocorrelation of ultrashort light pulses, Appl. Opt. 37 (1998) 8142–8144.
[14] M. Rasmusson, A.N. Tarnovsky, E. Akesson, V. Sundstrom, On the use of two-photon absorption for determination of femtosecond pump probe cross correlation functions, Chem. Phys. Lett. 335 (2001) 201–208.
[15] D.J. Bradley, H.C. Geoffrey, Ultrashort pulse measurements, Proc. IEEE 62 (1974) 313–345.
[16] O. Ollikainen, A. Rebane, D. Erni, U.P. Wild, Femtosecond time-resolved pulse measurement and image detection in broad spectral range by two-photon-excited fluorescence, Lasers Electro. Opt. (1996) 227–228.
[17] O. Lammel, A. Penzkofer, Femtosecond pulse duration measurement by two photon fuorescence detection, Opt. Quantum Electron. 32 (2000) 1147–1160.
[18] P. Sperber, A. Penzkofer, Pulse-shape determination of intracavity compressed picosecond pulses by two-photon fluorescence analysis, Opt. Quantum Electron. 18 (1986) 145–154.
[19] N.K.M. Naga Srinivas, S. Venugopal Rao, D. Narayana Rao, Saturable and reverse saturable absorption of Rhodamine B in methanol and water, JOSA Soc. Am. B 20 (2003) 2470–2479.